

*Full Research Paper*

## **Investigation on Clarified Fruit Juice Composition by Using Visible Light Micro-Raman Spectroscopy**

**Carlo Camerlingo**<sup>1</sup>, **Flora Zenone**<sup>2,3</sup>, **Ines Delfino**<sup>4</sup>, **Nadia Diano**<sup>3,5</sup>,  
**Damiano Gustavo Mita**<sup>3,5\*</sup> and **Maria Lepore**<sup>3,5</sup>

1 Consiglio Nazionale delle Ricerche, Istituto di Cibernetica “E. Caianiello”, Pozzuoli, Italy

2 Dipartimento di Scienze Fisiche, Università “Federico II”, Naples, Italy

3 Consorzio Interuniversitario INBB, Sezione di Napoli, Italy

4 Biophysics and Nanoscience Centre, CNISM, Università della Tuscia, Viterbo, Italy

5 Dipartimento di Medicina Sperimentale, Seconda Università di Napoli, Naples, Italy

\* Author to whom correspondence should be addressed. E-mail : mita@igb.cnr.it

*Received: 21 September 2007 / Accepted: 1 October 2007 / Published: 3 October 2007*

---

**Abstract:** Liquid samples of clarified apple and apricot juices at different production stages were investigated using visible light micro-Raman spectroscopy in order to assess its potential in monitoring fruit juice production. As is well-known, pectin plays a strategic role in the production of clarified juice and the possibility of using Raman for its detection during production was therefore evaluated. The data analysis has enabled the clear identification of pectin. In particular, Raman spectra of apple juice samples from washed and crushed fruits revealed a peak at  $845\text{ cm}^{-1}$  (typical of pectin) which disappears in the Raman spectra of depectinised samples. The fructose content was also revealed by the presence of four peaks at  $823\text{ cm}^{-1}$ ,  $872\text{ cm}^{-1}$ ,  $918\text{ cm}^{-1}$  and  $975\text{ cm}^{-1}$ . In the case of apricot juice, several Raman fingerprints of  $\beta$ -carotene at  $1008$ ,  $1159$  and  $1520\text{ cm}^{-1}$  were also highlighted. Present results resulted interesting for the exclusive use of optical methods for the quantitative determination of the above-mentioned substances in place of the biochemical assays generally used for this purpose, which are time consuming and require different chemical reagents for each of them.

**Keywords:** Fruit juice, Micro-Raman Spectroscopy, Pectin, Pectinase, Apple, Apricot

---

## 1. Introduction

In the present paper it is described the application of visible micro-Raman spectroscopy to the characterization of liquid samples of clarified apple and apricot juices at different production stages during the tests in a pilot plant of an integrated membrane process recently proposed by S. Alvarez et al [1]. Micro-Raman spectroscopy was performed without any preliminary treatment of juice samples and by using a visible laser source. In this way we exploited the possibility of using Raman spectroscopy for on-line monitoring the production of clarified fruit juices, with appealing perspectives for a real-time control of the process and of the juice quality as concern, for instance, the pectin, fructose or  $\beta$ -carotene content. As a consequence of significant improvements of micro-Raman spectroscopy technology, an increasing attention has been given to the applications of Raman spectroscopy to heterogeneous systems such as those used in the food industry [2,3]. Raman spectroscopy has been successfully employed in the characterization of starch and pectin in potato [3], bitter almonds [4] and for edible oil authentication [5]. In particular, powdered pectin has been extensively investigated by means of FT-IR and FT-Raman spectroscopy [6]. FT-Raman spectroscopy allows a clear distinction to be made between different kinds of sugars [7] and therefore has been used to differentiate honey from various regions [8]. Almost all these studies have been carried out with FT-Raman spectroscopy by using near infrared excitation sources to avoid the fluorescence emission, typical of many biological samples. However, the possibility of heating the samples with these laser sources should be considered despite the brevity of data acquisition time and the laser exposure times nowadays currently used. It should also be noted that powdered samples were considered in all cases, even though Raman spectroscopy was already adopted to quantify different analytes in solution [9]. It can be worthwhile to remember that water, present in high concentrations in fruits and in many food products, constitutes a severe limit for FT-IR owing to its high IR light absorption coefficient, while it has a weak Raman signal and usually does not interfere with the spectra of other components.

All these considerations motivated us to develop a friendly-to-use experimental procedure that by using micro-Raman spectroscopy allowed us to monitor the pectin, fructose and  $\beta$ -carotene contents in clarified fruit juice production. It is also important to remember that biochemical assays generally used to quantify the above-mentioned substances are time consuming and require the use of different chemical reagents for each component, so the results reported here suggest that the role of Raman spectroscopy can be of valuable interest also for off-line quantitative monitoring.

## 2. Materials and Methods

### 2.1 Materials

The composition of a fruit juice depends on the variety, origin and growing conditions of the fruit, its quality and the processing and storage procedures. Excluding water, the major components of fruit juices are carbohydrates, acids, nitrogen compounds, polyphenols, minerals and vitamins. As an example, Table 1 shows the approximate composition of raw apple juice obtained after pressing apples [10]. Recently clear and filtered juices have become more popular with respect to hazy, unfiltered and unclarified juices, traditionally produced. If a cloudy product is required, the juice is pasteurised immediately after pressing in order to denature any residual enzymes. Centrifugation then removes

large pieces of debris, leaving most of the particles in suspension. To obtain a clear juice these suspended particles need to be removed. They could simply be filtered out, but unfortunately some soluble pectin remains in the juice, making it too viscous to filter quickly. Enzymatic treatment with pectinase is the adopted method for removing unwanted pectin. Pectinase is a balanced mix of pectolytic enzymes designed to provide controlled maceration and depectinization of fruit. It contains high levels of pectin lyase (PL), which depolymerizes pectin chains, and polygalacturonase (PG), which randomly cuts the polygalacturonic acid backbone of the insoluble pectin.

**Table 1.** Approximate composition of apple juice components. For each compound the correspondent concentration (g/l) contained in apple juice is reported.

Compound	Concentration (g/l)
Water	860-900
Sugars	100-120
Fructose	46-70
Sucrose	27
Glucose	20
Malic acid	3-7
Pectin	1-5
Starch	0.5-5
Polyphenols	1
Proteins	0.6
Vitamins (mainly ascorbic acid)	0.05
Ashes	2

The low levels of pectin methylesterase (PME) ensures that only minimal levels of methanol are produced by the demethylation of pectin. Four different types of samples, identified as A, B, C and D, were examined in this investigation. As reported in the introduction these samples were produced at different stages during the tests in a pilot plant of an integrated membrane process. Samples of type A were made of apple juice extracted from washed and crushed fruit, after pre-press treatment with a small percentage of (Macer8™ FJ, Biocatalysts, Cardiff, UK) pectinase which was added to allow the juice to flow more easily. This treatment has an insignificant effect on the amount of pectin present in the juice. Samples of type B were obtained from apple juice taken from the production line after depectinisation done using immobilized pectinase. Samples of type C were taken from apricot juice treated in the same way as sample of type A. Samples of type D were powdered pectin (from Unipectine from Crestchen Ltd., Buckinghamshire, England) diluted in deionized water and were examined in order to obtain reference spectra.

## 2.2 Methods

### 2.2.1 Raman spectroscopy measurements

Raman spectroscopy provides information about molecular structure and, by combining spectroscopy with microscopy, qualitative and quantitative information can be obtained in a non-invasive way. This method is a very effective tool in food analysis because it is non-destructive and usually requires no special preparation of the sample.

The process of Raman scattering can be viewed as an inelastic scattering process in which the scattered photon is shifted in frequency from the incident photon as it either loses energy to or gains energy from a particular vibrational mode of the molecule [11]. Raman is a specific spectroscopic technique that measures the fundamental vibrations of functional groups that can be employed to determine the chemical structure and dynamics of molecules of interest. For more detailed description of the physics of Raman effect see ref. [12].

Our samples were excited by a *He-Ne* laser operating at a wavelength  $\lambda = 633$  nm, with a maximum nominal power of 17 mW. The laser light was focused on the sample surface by means of a 50 $\times$  optical objective (Olympus MPLAN 50 $\times$ /0.75) or a 20 $\times$  long distance objective (Olympus MPLAN 20 $\times$ /0.35) on an excitation area of about 20 $\times$ 20  $\mu\text{m}^2$  or 50 $\times$ 50  $\mu\text{m}^2$ , respectively. The micro-Raman spectrometer was equipped with an optical confocal microscope (Olympus BX40) connected by a 50  $\mu\text{m}$  optical fibre to a Jobin-Yvon TriAx 180 monochromator with liquid nitrogen-cooled CCD detector. Three gratings of 300, 600 and 1800 grooves/mm were selectable, allowing a maximum spectral wavenumber resolution of 4  $\text{cm}^{-1}$ . The highest resolution grating (1800 grooves/mm) was generally used, except when the acquisition of a large spectrum range was required. In this case the 600 grooves/mm grating was used. The spectra were obtained using accumulation times ranging from 60 to 300 s by means of a double acquisition process which permits the rejection of spurious peaks due to direct CCD excitations. Small amounts of samples A, B, C and D were examined using the above-described micro-Raman spectrometer equipment. A drop of the liquid sample of a few milliliters was placed on a microscope glass slide with a single well (1 cm large and 0.1 cm depth) suitable for investigating liquid specimens. A cover glass (170  $\mu\text{m}$  thick) was placed on the top of the concavity to avoid contamination of the optical objective. For each kind of sample experimental analysis was performed more times and on different drops of the same juice in order to test the representivity and reproducibility of the measure. Since our measurements were carried out on liquid samples, they were affected by scattering and optical aberration effects due to the water and other scattering elements, which reduce the quality of recorded spectra. Therefore, it was difficult to extract quantitative information from the spectral data [13]. Nevertheless, using high optical aperture objectives (as in the case of the objective 50 $\times$ ) and appropriately setting the laser focus, a reproducible Raman response was obtained. Even if the total collected signal was decreased when confocal microscopy was used, this technique improved the readability of micro-Raman signal, limiting the reflected light component out-of-focus and, consequently, reducing the signal noise in the spectra. In our measurements the confocal pinhole was fixed to values in the range of 200  $\mu\text{m}$  - 500  $\mu\text{m}$ , depending on the experimental light reflection conditions.

## 2.2.2 Biochemical assays

### 2.2.2.1 Pectin content

Following the procedure given by Bernfeld [14] pectin was assayed by spectrophotometrically measuring at 530 nm the reducing groups. The maximum value of pectin content in the initial stage of production was found to be 5% (w/w). This value was found to decrease during the subsequent production steps. For daily and qualitatively control we used the most easily to use “acidified alcohol test” [15]. It is very common in fruit juice industry and exploits the formation of a viscous gel when pectin reacts with ethanol acidified with chlorhydric acid.

### 2.2.2.2 Fructose content

For fructose we referred to Youn et al [16] who assessed a content varying from 6.36 to 7.15 % for clarified apple juice samples at different stages of membrane filtration processes.

### 2.2.2.3 $\beta$ -Carotene content

Usually the determination of  $\beta$ -carotene content is performed following the method of Stahl et al [17]. For apricot fruit juice a  $\beta$ -carotene content around 33.8  $\mu\text{g/g}$  is found from literature [18].

## 2.2.3. Data analysis

The spectra were analyzed using the application routines given by the same software package (“SpectraMax™ Software” user guide, Joben-Yvon Inc. USA) controlling the whole data acquisition system. In doing so, extremely rapid and versatile on-line data processing is required. In particular, the above-mentioned software enabled us both to remove fluorescence by correcting the baseline, using different polynomial models, and to analyse the complex spectra in terms of convoluted Lorentzian-shaped vibrational modes. Peaks, constituting the spectrum, were manually selected in order to define the starting conditions for a best-fit procedure. The best-fit program can then be repeated to determine convolution peaks with optimised intensity, position and width. The performance was evaluated by means of the  $\chi^2$  parameter defined as usual by the following formula:

$$\chi^2 = \frac{\sum_{i=0}^n \left( \frac{\text{Actual}_i - \text{Calculated}_i}{\text{RMSNoise}} \right)^2}{(n - f)}$$

The *Actual* and *Calculated* values refer to the measured and calculated data, respectively. The *RMSNoise* is the estimated Root Mean Square noise in the *Actual* data over the fitted region. The variable *n* refers to the number of data points in the fitted region while *f* refers to the total number of variables from the peak and baseline functions. Thus, *n-f* is the number of degrees of freedom. The

Levenberg-Marquardt algorithm iteratively adjusts every variable for each peak in an attempt to minimize the  $\chi^2$  parameter. This kind of algorithm is extremely useful for determining the exact peak positions, widths, heights and areas of a set of overlapping peaks.

### 3. Results and Discussion

Figure 1 shows the micro-Raman spectrum of a sample of type A, i.e. apple juice before depectinisation. The spectrum was measured on a broad wavenumber shift range (from 200 to 3200  $\text{cm}^{-1}$ ). As no significant Raman signals were found in the region between 2000  $\text{cm}^{-1}$  and 2500  $\text{cm}^{-1}$ , only the two regions (200- 2000  $\text{cm}^{-1}$ ) and (2500-3200  $\text{cm}^{-1}$ ) are reported. The qualitative features of this spectrum are representative of all the spectra obtained for the samples currently being investigated. They show a featureless background beneath specific narrow bands, suggesting the presence of fluorescence signals and scattering effects, which are typical when liquid fruit juice samples are examined, despite the care adopted during the measurements. The signal-to-noise-ratio of Figure1 is considerably lower than that typically featured by spectra acquired from solid samples by means of the same apparatus [19]. It is worth emphasizing that the spectrum shown in Figure1 was obtained from untreated liquid samples and by using a visible light in micro-Raman apparatus, which are two key requirements to make Raman spectroscopy suitable for large industrial applications.

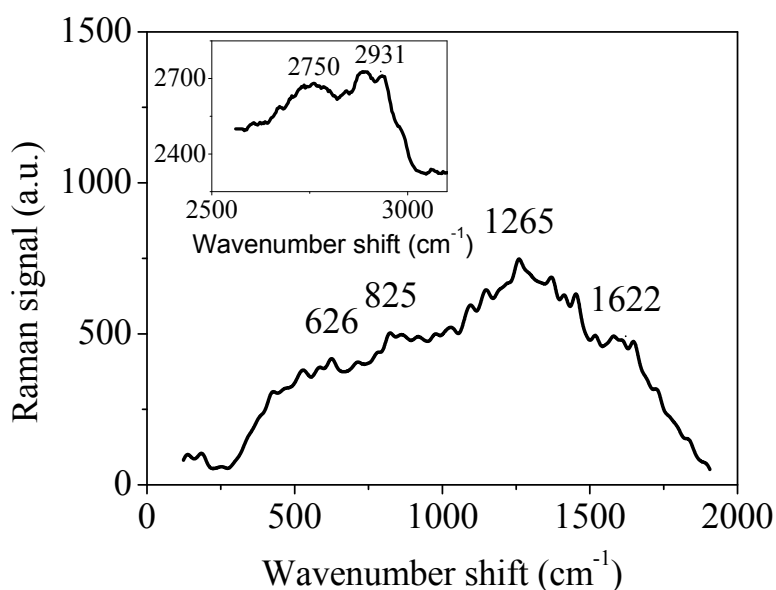


**Figure 1.** Raman spectrum measured on a fruit juice sample of type A (apple juice). The investigated wavenumber shift range varies between 200 and 3200  $\text{cm}^{-1}$ .

However, in spite of the low signal level, a considerable amount of information can be extracted from liquid sample-related Raman spectra. Indeed, a preliminary examination of this figure evidences some structures around 626, 825, 1265, 1622, 2750 and 2931  $\text{cm}^{-1}$ . The bands at 626 and 1265  $\text{cm}^{-1}$  can be assigned to fructose and the one at 825  $\text{cm}^{-1}$  to the furanose isomer of fructose [20]. The structures at 1622  $\text{cm}^{-1}$  and around 2700-2900  $\text{cm}^{-1}$  can be assigned to in-plane bending of amide II and

to the stretching of the C-H aliphatic group of pectin [21]. The previously described data analysis procedure was applied to a portion of the above-mentioned spectrum that is shown in the upper part of Figure 2 (Figure 2a) for the 700-1200  $\text{cm}^{-1}$  range. In the same part of the figure, the result of the curve fitting procedure is shown as a continuous thick line. In the middle part of the figure (Figure 2b), the peaks used are reported and information about their exact positions, widths, heights and areas is provided by the program. In the lower part of the figure (Figure 2c), the residual error, i.e. the uncorrelated signal resulting from the subtraction of fit curve from the acquired Raman signal, is shown. It remains very close to zero throughout the examined spectral region (see the scale on the left) making us confident that the number and characteristics of peaks are almost sufficient in this preliminary analysis of the data. It is worthwhile to note that in the examined range the analysis has allowed us to single out the presence of other structures in addition to the one at 825  $\text{cm}^{-1}$  that been already assigned to the furanose isomer of fructose. The peaks coming out from deconvolution are located at 780, 845, 872, 918, 975, 1031, 1061, 1083  $\text{cm}^{-1}$ . The tentative assignment of these peaks is reported in Table 2. From this table it is possible to affirm that Raman spectra allows us to detect the presence of few percents of pectin and fructose according to the results of biochemical assays previously reported.

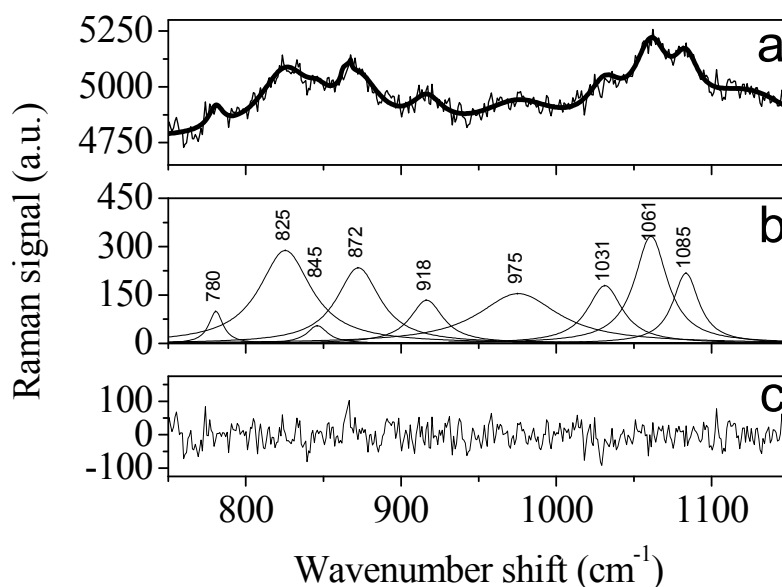


**Figure 2.** Deconvolution procedure on the spectrum reported in Figure 1 in the wavenumber range 700-1200  $\text{cm}^{-1}$ . The continuous upper curve (a) represents the best fit using the components shown in the frame (b). The curve in (c) represents the residual errors for the fit (see the scale on the right).

**Table 2.** Tentative assignment of the main peaks in Raman spectrum of apple fruit juice in the range 700 – 1200 cm<sup>-1</sup>

Peak wavenumber (cm <sup>-1</sup> )	Pectin	Fructose	Ref.
825		furanose isomer	20
845	C-O-C antisymmetric stretching of the glycoside linkage		3, 21
872		furanose isomer	20
918	In-plane bending of CH <sub>2</sub>	furanose isomer	20
975		pyranose isomer	20
1031			21
1061	Nonlocalized, highly coupled vibrational modes of polysaccharide backbones		21
1083		C-O stretching	20

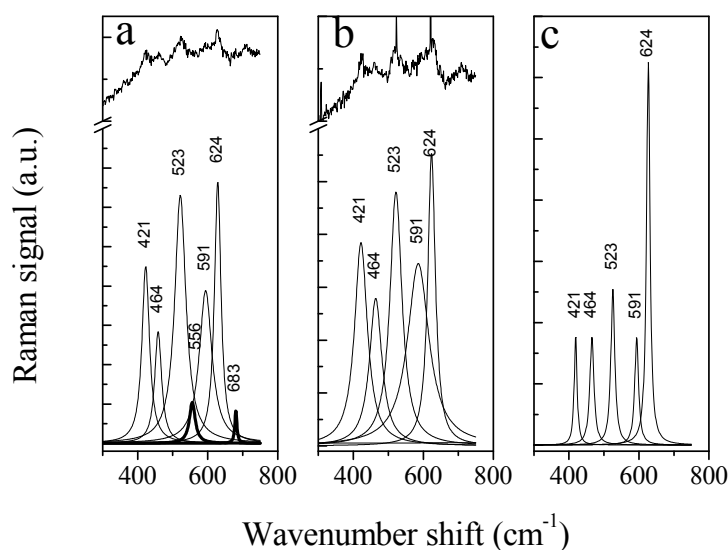
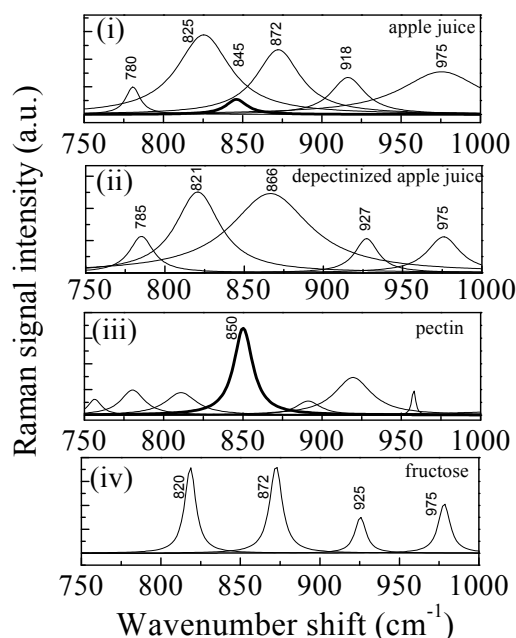
**Figure 3.** Comparison of Raman spectra in the 300-750 cm<sup>-1</sup> range of : (a) apple juice of type A (before depectinisation) , (b) apple juice of type B (after depectinisation) and (c) fructose (Ref. 22).

Figure 3 shows the results of the above-described data procedure for the spectra of samples of type A (panel a), type B (panel b), and fructose [22] (panel c) in the wavenumber shift range 300-750 cm<sup>-1</sup>. In the panel a the deconvolution of the experimental spectrum (upper curve) can be used to evaluate the contribution of seven peaks which are centered at 421, 464, 523, 537, 591, 624 and 683 cm<sup>-1</sup>, respectively. In the central panel (b), related to depectinised fruit juice, five peaks, centered at 421, 464, 523, 591, 624 cm<sup>-1</sup>, are evident. As it is clear from the panel c, these peaks can be ascribed to fructose. More precisely, the peak at 464 cm<sup>-1</sup> may be due to the furanose isomer and the peaks at 421



and  $523\text{ cm}^{-1}$  can be related to the pyranose [20]. Conversely, the two peaks at  $537$  and  $683\text{ cm}^{-1}$  due to pectin (following ref. 21) are no longer present. Obviously, in this case and in all the other cases reported here, we checked that the values of the residual errors always were very close to zero. Also in this case the absence of pectin was qualitatively confirmed by the acidified alcohol test.

A similar example of the potentiality of Raman measurements is shown in Figure 4. This figure illustrates the results obtained using the same procedure for the wavenumber range  $750 - 1000\text{ cm}^{-1}$  when applied to samples of A and B kind. In the panel (i) (apple juice prior to depectinisation) the peaks at  $780$ ,  $825$ ,  $845$ ,  $872$ ,  $918$  and  $975\text{ cm}^{-1}$  already evidenced in Figure 1 are present (for the assignment see Table 2). In the inset (ii) (apple juice after depectinisation) the same peaks are exhibited with the exception of the peak at  $845\text{ cm}^{-1}$ . This peak is typical of pectin [3, 21] and is clearly observable in the panel (iii) where the deconvolution of the spectrum directly acquired from pectin is shown. This peak is highly reproducible and can be ascribed to the C-O-C antisymmetric stretching of the glycoside linkage. In the panel (ii) there is no evidence of this peak. The lack of an  $845\text{ cm}^{-1}$  peak in the panel (ii) confirms the success of the depectinisation procedure and is also proved by the acidified alcohol test. The other peaks found in the sample A and B spectra can mainly be ascribed to the fructose contribution as is evident from panel (iv) which shows the deconvolution of the pure fructose spectrum [20]. In the panel (iv) we observe peaks at  $820$ ,  $872$ ,  $925$  and  $975\text{ cm}^{-1}$  which are also clearly present in the panels (i) and (ii). In particular, the peaks at  $820$  and  $975\text{ cm}^{-1}$  can be ascribed to pyranose isomer, while the structures at  $872$  and  $918\text{ cm}^{-1}$  can be assigned to furanose isomer [20].



**Figure 4.** Comparison of Raman spectra of apple juice sample of types A (i) and B (ii) (before and after depectinisation) with those of pectin (sample D) (iii) and fructose (iv) in the  $750 - 1000\text{ cm}^{-1}$  wavenumber shift range.

In the upper part of Figure 5, the typical spectrum of apricot juice samples before depectinisation is reported for the wavenumber range from  $800$  to  $1600\text{ nm}$ . Looking at this spectrum, the main

structures are highlighted and when the deconvolution procedure is applied we singled out the contribution made by pectin, fructose and  $\beta$ -carotene as shown in the curves in the lower part of the figure.

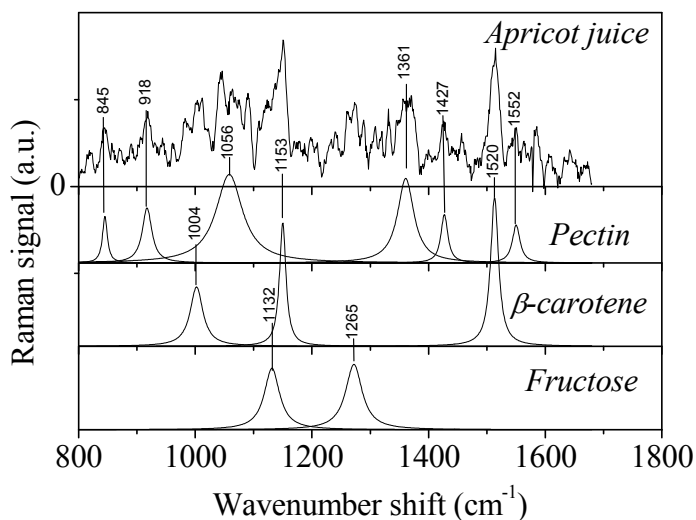


**Figure 5.** Results of deconvolution procedure on Raman spectrum of apricot juice (Sample C) before depectinization process and comparison with pectin,  $\beta$ -carotene and fructose spectra.

**Table 3.** Tentative assignment of the main peaks in Raman spectrum of apricot fruit juice in the 800-1600  $\text{cm}^{-1}$  range

Peak wavenumber ( $\text{cm}^{-1}$ )	Pectin	Fructose	$\beta$ -carotene	Refs.
845	C-O-C antisymmetric stretching of the glycoside linkage	-	-	21
918	In-plane bending of $\text{CH}_2$	Furanose isomer	-	20
1004	-	-	Methyl component rocking	23
1056	Nonlocalized, highly coupled vibrational modes of polysaccharide backbones	-	-	21
1132	-	Pyranose isomer	-	20
1153	-	-	C-C stretching	23
1265	-	D- fructose	-	20
1361	C-H bending	-	-	21
1427	$\text{COO}^-$ symmetric stretching	-	-	21
1520	-	-	C=C stretching	23
1552	Amide II: N-H deformation Contribution from C-N stretching	-	-	21

In Table 3 the assignments of these peaks taken from literature [20-24] are tentatively reported. From the table it can be concluded that only in the case of the structure around  $820 \text{ cm}^{-1}$  there is a contribution from pectin and fructose, while in all other cases the assignments would seem to be

unambiguous. Also for  $\beta$  - carotene it is possible to say that the micro-Raman spectroscopy is able to detect the presence of carotene, that was confirmed by biochemical assays [18].

#### 4. Conclusions

All the results reported here demonstrate that visible light micro-Raman spectroscopy can be successfully adopted in order to investigate the composition of fruit juice liquid samples. Generally to obtain useful Raman spectra from liquid heterogeneous samples is often difficult and many samples are therefore dried before being measured. Furthermore, it is necessary to employ infrared laser sources in order to reduce fluorescence effects. In the present case, the use of confocal geometry enabled us to obtain informative Raman spectra by means of a less expensive visible light apparatus. In addition by using confocal geometry, extremely small volumes are sampled minimizing scattering and fluorescence effects. Moreover, useful information by using the application routines available from the software package controlling our data acquisition system can be obtained. Indeed, the contribution of three important fruit juice components was clearly revealed.

This would allow us to employ Raman spectroscopy for direct on-line monitoring of pectin, fructose and  $\beta$ -carotene content in liquid fruit juice samples at different production stages without pre-treatment. Micro-Raman spectroscopy therefore proves to be an alternative or complementary technique to the turbidity measurements usually adopted in the food industry (see, for example, web site <http://www.themcnab.com>) in beer production, water monitoring etc. . Obviously, the possibility of extending the application of Raman techniques in on-line monitoring juice production processes significantly improves the effectiveness of the monitoring process. Indeed, besides detecting unwanted particles, as in the case of turbidity measurement, Raman spectroscopy provides information about their biochemical characteristics. The potential applications of Raman spectroscopy in the food industry could be increased if a quantitative determination of unwanted particles can be extracted by recorded spectra by developing multivariate analysis procedures [25]. These procedures will be also interesting for off-line analysis since biochemical assays generally used to quantify pectin, fructose and  $\beta$ -carotene contents are generally time consuming and require the use of different chemical reagents.

#### References

1. Alvarez, S.; Riera, F.A.; Alvarez, R.; Coca, J.; Cuperus, F.P.; Bouwer, S. Th.; Boswinkel, G.; van Gemert, R.W.; Veldsink, J.W.; Giorno, L.; Donato, L.; Todisco, S.; Drioli, E.; Olsson, G. Tragardh; J., Gaeta; S.N.; Panyor, L. A new integrated membrane process for producing clarified apple juice and apple juice aroma concentrate. *Journal of Food Engineering* **2000**, *46*, 109-125.
2. Li Chan, E.C.Y. The Application of Raman Spectroscopy in Food Science. *Trends in Food Science & Technology* **1996**, *7*, 361-370.
3. Thygesen, L.G.; Lokke, M.M.; Micklander, E.; Engelsen, S. B. Vibrational microspectroscopy of food. Raman vs FT-IR. *Trends in Food Science & Technology* **2003**, *14*, 50-57.
4. Micklander, E.; Brimer, L.; Engelsen S.B. Non-invasive assays for cyanogenic constituents in plants by Raman spectroscopy: contents and distribution of amygdalin in bitter almond. *Applied Spectroscopy* **2002**, *56*, 1139-1146.

5. Baeten, V.; Dardenne, V.; Aparicio, R. Interpretation of Fourier-Transform Raman spectra of the unsaponifiable matter in a selection of edible oils. *J. Agric. and Food Chemistry* **2001**, *49*, 5098-5107.
6. Synytsya, A.; Copíková, J.; Matejka, P.; Machovic V. Fourier-Transform Raman and infrared spectroscopy of pectins. *Carbohydrate Polymers* **2003**, *54*, 97-106.
7. Goral, J.; Zichy V. Fourier-Transform Raman Studies of Materials and Compounds of Biological Importance. *Spectrochimica Acta* **1990**, *46A*, 253-275.
8. Goodacre, R.; Radovic, B.S.; Anklam E. Progress toward the rapid non-destructive assessment of the floral origin of European honey using dispersive Raman spectroscopy. *Applied Spectroscopy* **2002**, *56*, 521-527.
9. Berger, A.J.; Itzkan, I.; Feld, M. Feasibility of measuring blood glucose concentration by near-infrared Raman spectroscopy. *Spectrochim. Acta Part A* **1997**, *53*, 287-292.
10. National Centre for Biotechnology Education. In a jam and out of juice. *NCBE - Practical protocol* 2000 ISBN 0 7049 13739, U.K.
11. Raman, C. V.; Krishnan, K. S. A New Type of Secondary Radiation. *Nature* **1928**, *121*, 501-502.
12. Lewis, I. R.; Edwards H.G.M. Handbook of Raman Spectroscopy. New York 2001: Marcel Dekker Inc.
13. Aarnoutse, P. A.; Westerhuis J. A. Quantitative Raman Reaction Monitoring Using the Solvent as Internal Standard. *Anal. Chem.* **2005**, *77*, 1228- 1236.
14. Bernfeld, P. Amylase a and b *Methods in Enzymology* **1955**, *1*, 149-150.
15. Grassin, C.; Fauquembergue, P. *Progress in Biotechnology 14: Pectins and pectinases*. Visser J., Voragen A.G.J. (eds), 1996 , Elsevier, Amsterdam, 453–463.
16. Youn, K.S.; Hong, J.H.; Bae, D.H.; Kim, S.J.; Kim, S.D. Effective clarifying process of reconstituted apple juice using membrane filtration with filter-aid pretreatment *Journal of Membrane Science* **2004**, *228*, 179-186.
17. Stahl, W.; Schwarz W.; Sies, H. Human serum concentrations of all-*trans*  $\beta$ - and  $\alpha$ -carotene but not 9-*cis*  $\beta$ -carotene increase upon ingestion of a natural isomer mixture obtained from *Dunaliella salina* (betatene). *J. Nutrition* **1993**, *123*, 847-851
18. Doker, O.; Salgin, U.; Sanal, I.; Mehentogh, U.; Calimli, A. Modeling the extraction of  $\beta$  - carotene from apricot bagasse using supercritical CO<sub>2</sub> in packed bed extractor. *Journal of Supercritical Fluids* **2004**, *28*, 11-19.
19. Camerlingo, C.; Delfino, I.; Lepore, M. Micro-Raman spectroscopy on YBCO films during heat treatments. *Supercond. Sci. Technol.* **2002**, *15*, 1606-1609.
20. Cerchiaro, G.; Sant'Ana, A.C.; Arruda Temperini, M.L.; da Costa Ferriera, A.M. Investigations of different carbohydrate anomers in copper(II) complexes with D-glucose, D-fructose, and D-galactose by Raman and EPR spectroscopy. *Carbohydrates Research* **2005**, *340*, 2352-2359.
21. Engelsen, S.B.; Noorgard L. Comparative vibrational spectroscopy for determination of quality parameters in amidated pectins as evaluated by chemometrics. *Carbohydrates Polimers* **1996**, *30*, 9-24.
22. Engelsen, S.B. Food Technology KVL. Database on Raman Spectra of Carbohydrates <http://www.models.kvl.dk/users/engelsen/specarb/fructose.html>.

23. Koyama, Y.; Takatsuka I.; Nakata M.; Tasumi M. Raman and infrared spectra of *all-trans*, *7-cis*, *9-cis* and *15-cis* isomers of  $\beta$ -carotene: key-bands distinguishing stretched or terminal-bent configuration from central-bent configurations. *J. Raman Spectrosc.* **1988**, *19*, 37-49.
24. Baranska, M.; Schulz, H.; Baranski, R.; Nothnagel, T.; Christensen L.P. In Situ Simultaneous Analysis of Polyacetylenes, Carotenoids and Polysaccharides in Carrots Roots. *J. Agric. Food Chem.* **2005**, *53*, 6565-6571.
25. Martens, H.; Noes T. *Multivariate Calibration*, Wiley: New York, 1993.

© 2007 by MDPI (<http://www.mdpi.org>). Reproduction is permitted for noncommercial purposes.